

Supplementary Information

Pressure effects on the thermal decomposition reactions: A thermo-kinetic investigation

Anuj A. Vargeese*

A. Theoretical background of kinetic analysis

Vyazovkin's non-linear integral Method

Vyazovkin's method is a non-linear integral isoconversional method which can be used for nonisothermal experiments. Vyazovkin's method provides more precise apparent activation energy values by performing numerical integration.^{1,2} The extent of conversion (α) was computed from the weight loss data using the reported standard method.³ A 0.025 increment in α was used to compute the E_α values from the nonlinear integral isoconversional method. However, for comparison and plotting, constant α values are shown at an interval of 0.05. For a set of 'n' experiments carried out at different heating rates, the apparent activation energy can be determined at any particular value of α by finding the value of E_α for which the given function, Eq. (1), is a minimum. The minimization procedure is repeated for each value of α to find the dependence of the apparent activation energy on the extent of conversion.

$$\sum_i^n \sum_{j \neq i}^n [I(E_\alpha T_{\alpha,i})\beta_j] / [I(E_\alpha T_{\alpha,j})\beta_i] = \min \quad (1)$$

$$\text{Where, } I(E,T) = \int_0^T \exp\left(-\frac{E}{RT}\right) dT \quad (2)$$

β in Eq. (2) represents the heating rates, and the indexes i and j denote the set of experiments performed under different heating rates, and n is the total number of experiments performed.

The third degree approximation (Eq. (3)) proposed by Senum and Yang⁴ was used in the present study to evaluate the integral Eq. (2).

$$f(x) = \frac{\exp(-x)}{x} \times \frac{x^2 + 10x + 18}{x^3 + 12x^2 + 36x + 24} \quad (3)$$

$$\text{Where, } x = \frac{E}{RT} \quad \text{and} \quad I(E,T) = \frac{E}{R} f(x) \quad (4)$$

MatLab 7.0.1 was used to perform the kinetic computations.

(1) Vyazovkin, S.; Dollimore, D. Linear and Nonlinear Procedures in Isoconversional Computations of the Activation Energy of Nonisothermal Reactions in Solids. *J. Chem. Inf. Comput. Sci.* **1996**, 36, 42–45.

(2) Vyazovkin, S. Evaluation of Activation Energy of Thermally Stimulated Solid-State Reactions Under Arbitrary Variation of Temperature. *J. Comput. Chem.* **1997**, 18, 393–402.

(3) Brown, M. E. *Introduction to Thermal Analysis: Techniques and Application*, Kluwer Academic Publishers, New York, 2001.

(4) Senum, G. I.; Yang, R. T. Rational Approximations of the Integral of the Arrhenius Function. *J. Therm. Anal.* **1977**, 119, 445–447.

B. Differential thermogravimetric curves for AP and APC

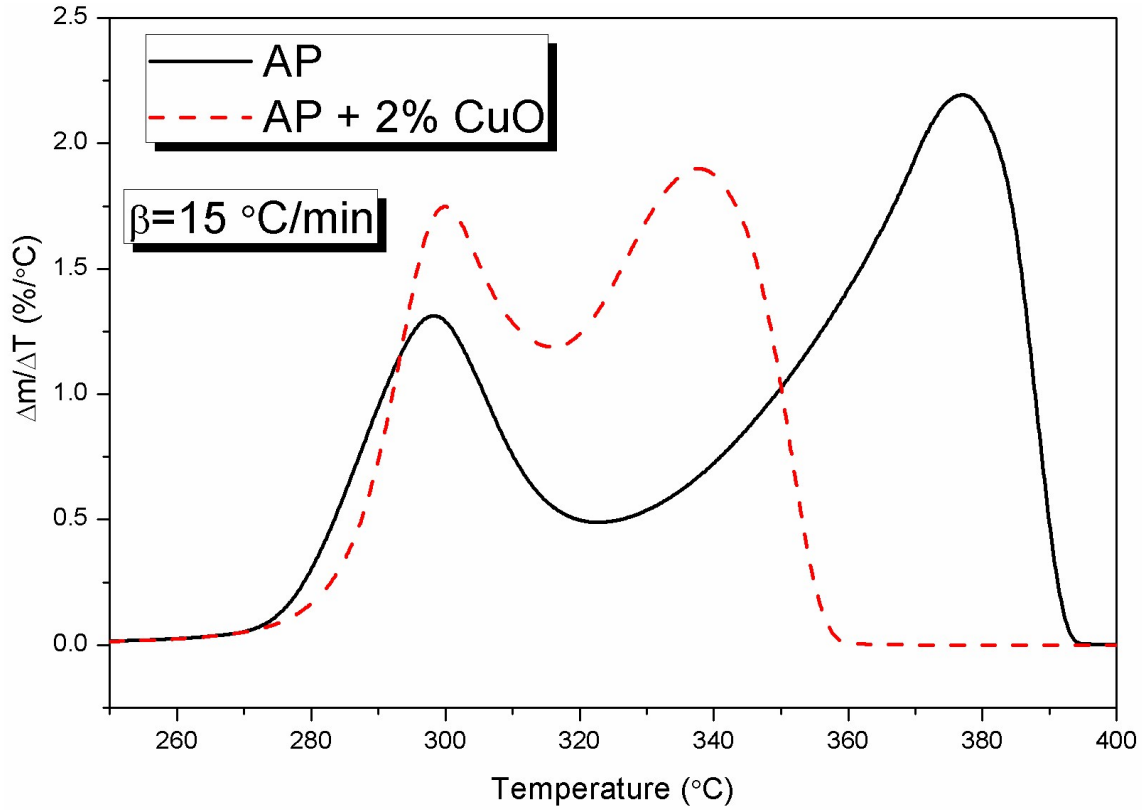


Figure 1. The differential thermogravimetric curves for AP and APC

C. DSC data

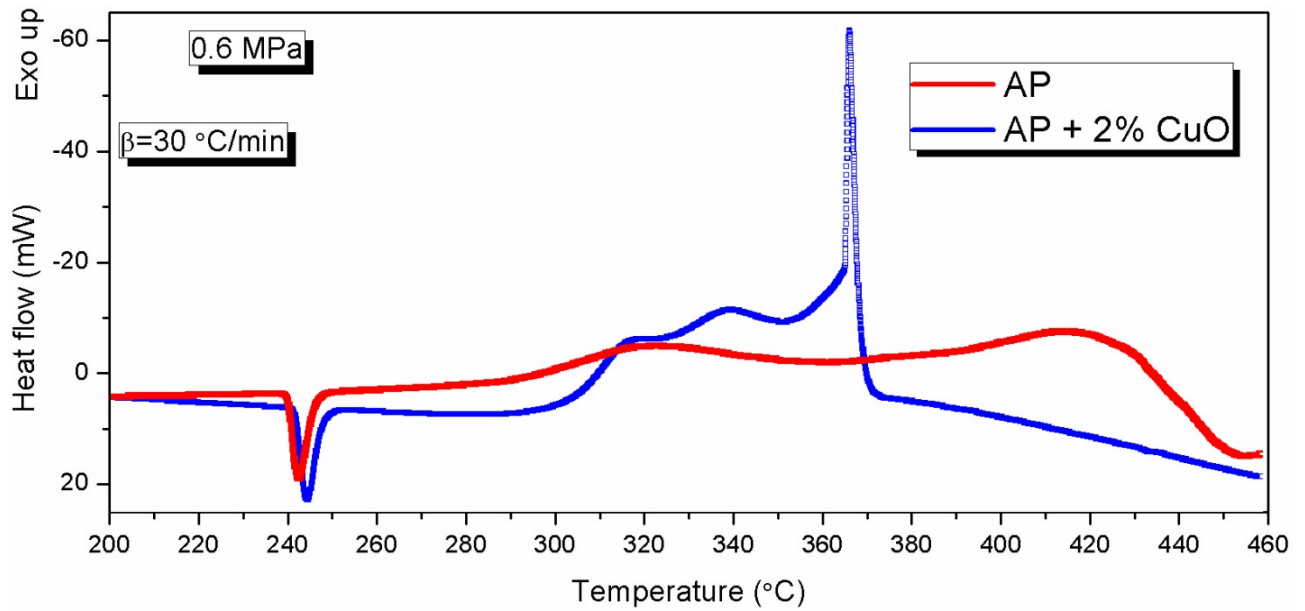


Figure 2. DSC curves obtained for AP and APC at 0.6 MPa

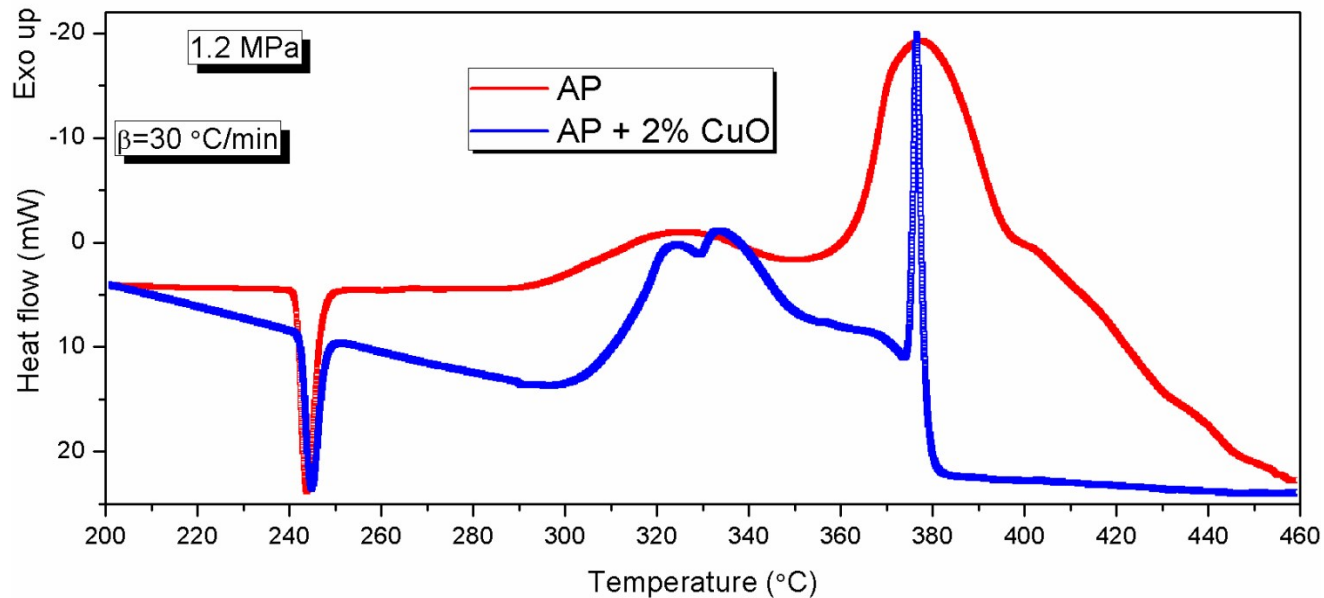


Figure 3. DSC curves obtained for AP and APC at 1.2 MPa

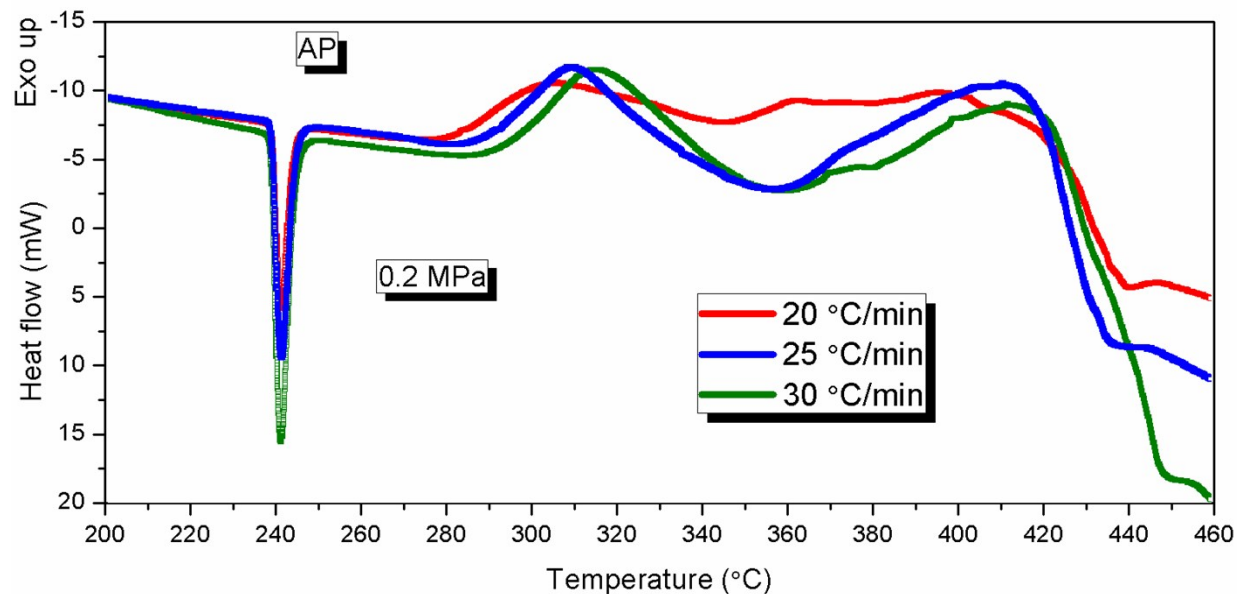


Figure 4. DSC curves obtained for AP (P=0.2 MPa) at three different temperatures (for kinetic analysis)

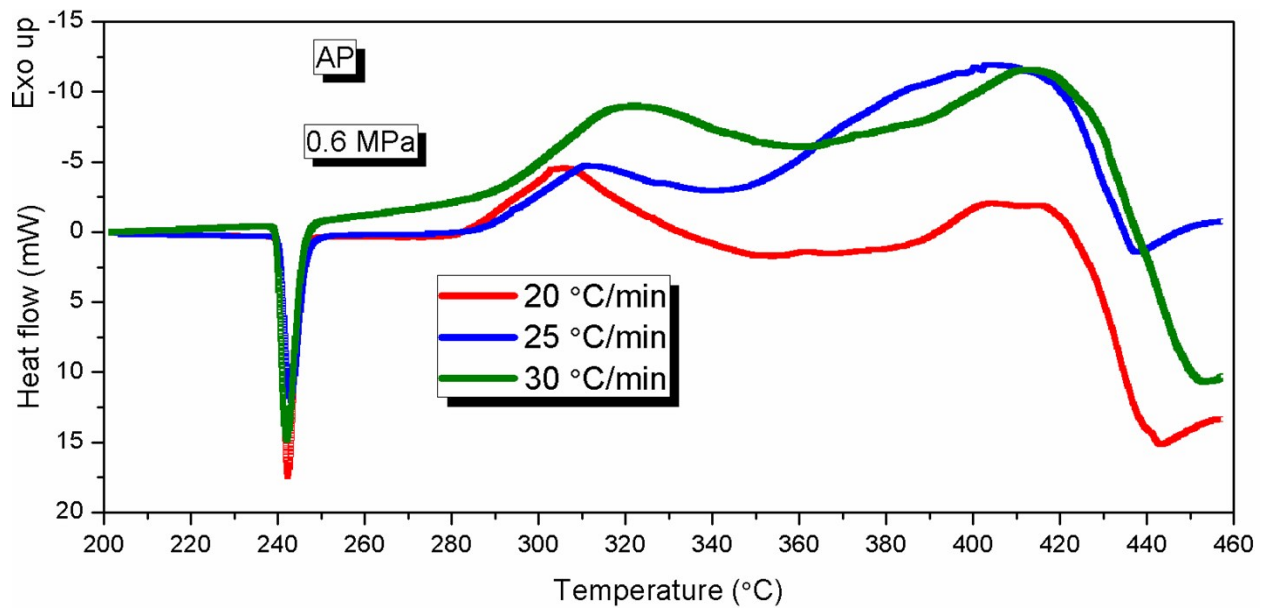


Figure 5. DSC curves obtained for AP ($P=0.6$ MPa) at three different temperatures (for kinetic analysis)

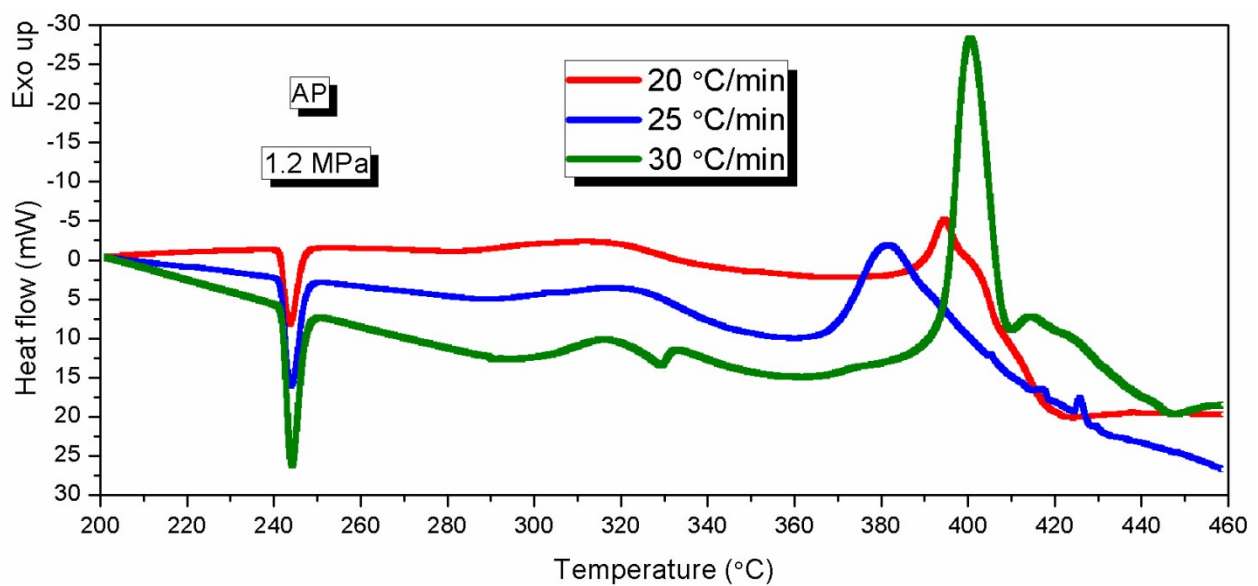


Figure 6. DSC curves obtained for AP ($P=1.2$ MPa) at three different temperatures (for kinetic analysis)

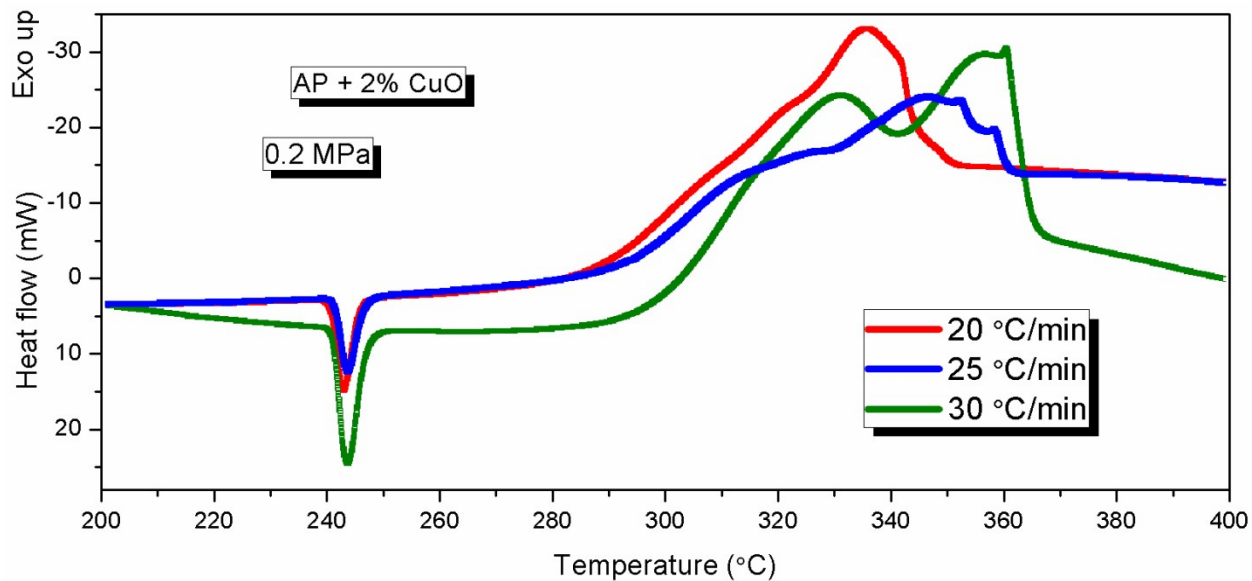


Figure 7. DSC curves obtained for APC (P=0.2 MPa) at three different temperatures (for kinetic analysis)

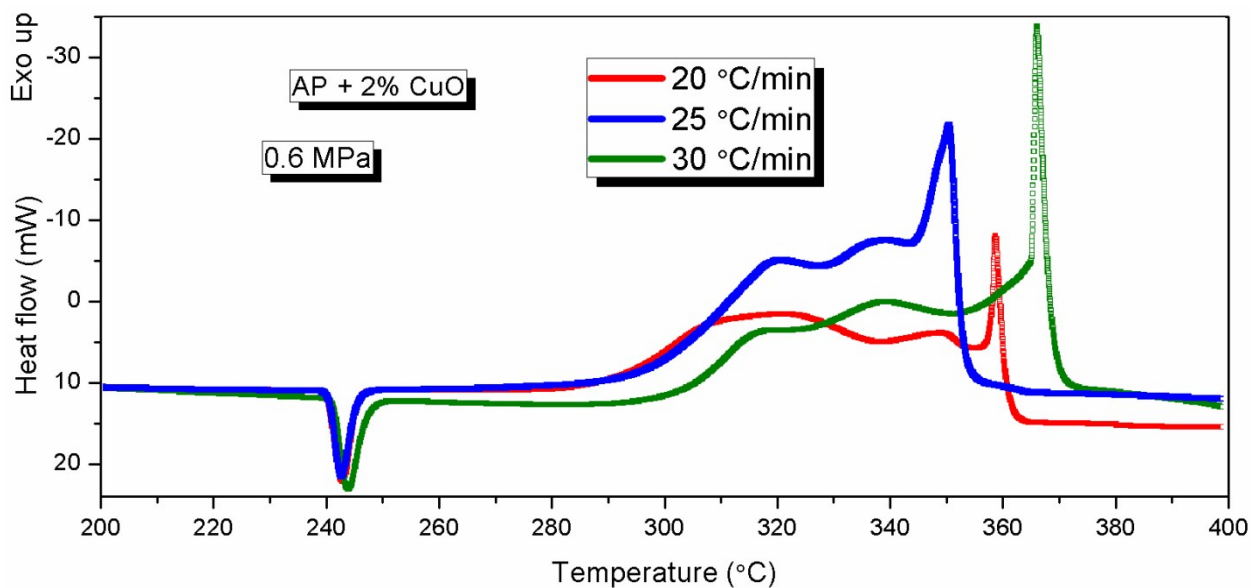


Figure 8. DSC curves obtained for AP (P=0.6 MPa) at three different temperatures (for kinetic analysis)

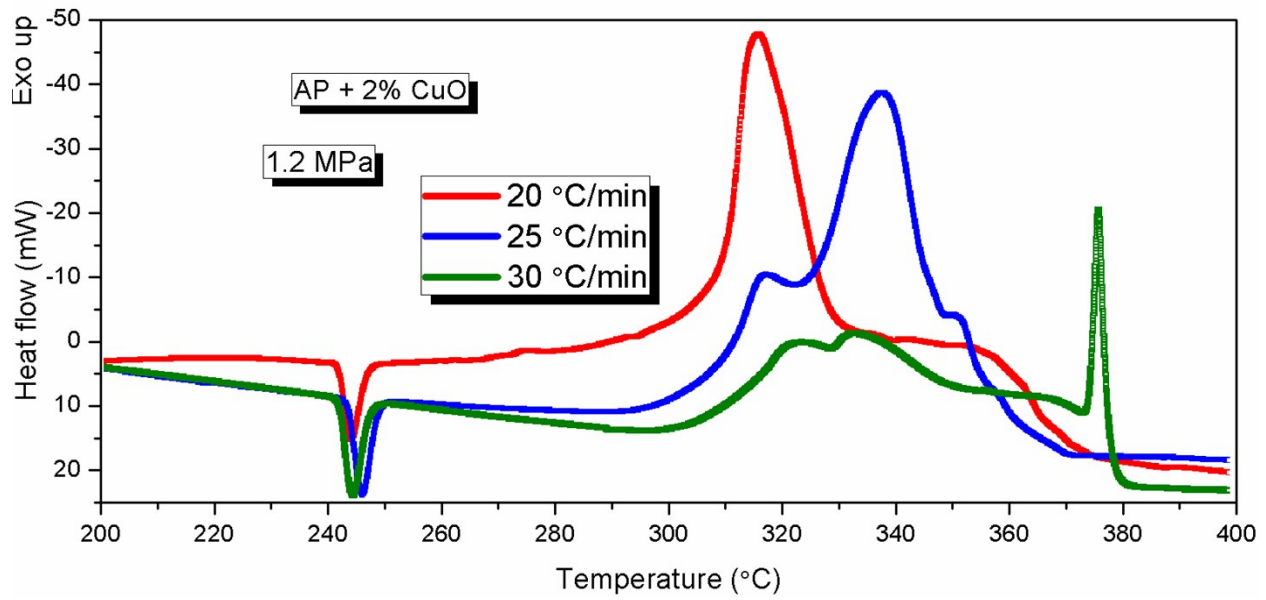


Figure 9. DSC curves obtained for APC (P=1.2MPa) at three different temperatures (for kinetic analysis)

D. CuO nanorod preparation and characterization

a. CuO nanorod preparation

10 mL aqueous solution (0.025 M) of copper acetate monohydrate ($\text{Cu}(\text{CH}_3\text{COO})_2 \cdot \text{H}_2\text{O}$) and urea were prepared separately and then mixed. The solution mixture was then transferred to a 20 mL Teflon-lined stainless steel pressure reactor. The pressure reactor was maintained at 130 °C for 1 h in a hot air oven and after the heat treatment, the pressure reactor was allowed to cool down to room temperature (~5-6 h). The product obtained after the reaction was washed several times with ethanol, collected through centrifugation and dried under reduced pressure and used for further analysis and application.

b. Characterization of CuO nanorod

The PXRD pattern was obtained using a 'Bruker D8 Advance' instruments at 30 °C and the sample was scanned over a 2θ range of 20–80°. A step size of 0.01° and a scan time of 1.5 s were used for the characterization of nanocatalyst. From the obtained PXRD patterns, the interplanar distances (d) were calculated by Bragg's equation and compared with the JCPDS data. SEM analysis was carried out by using a Carl - Zeiss (Model Ultra55) field emission scanning electron microscope (FESEM). The HRTEM study was carried out on a FEI Tecnai G² F20 S-Twin Transmission Electron Microscope. The samples for TEM analyses were obtained by diluting the dispersed solution with ethanol and then placing a drop (or two) of the diluted solution onto a Formvar covered copper grid and evaporated in air at room temperature. The FTIR spectrum of CuO nanorods dispersed in a KBR matrix (pellet) was recorded using a JASCO FTIR-5300. The TG

characterization was done on a TA instruments Q 600 SDTA with ~2 mg sample in a 90 μl crucible under flowing (100 mL/min) nitrogen atmosphere.

As shown in the SEM image (Fig. 10) the hydrothermal synthesis yields CuO microspheres with a diameter of approximately $1\mu\text{m}$. The TEM analysis further confirmed the formation of these microspheres as shown in Fig. 11. The sample was then subjected to ultrasonication and the TEM images were recorded for sample collected in between the process and after pro-longed exposure to ultrasonication. The Figure 2b shows images recorded for the sample collected in between the ultrasonication. The images indicated the formation of CuO microspheres with $1\mu\text{m}$ size and disintegration microspheres to form smaller particles and ultimately the CuO nanorods.

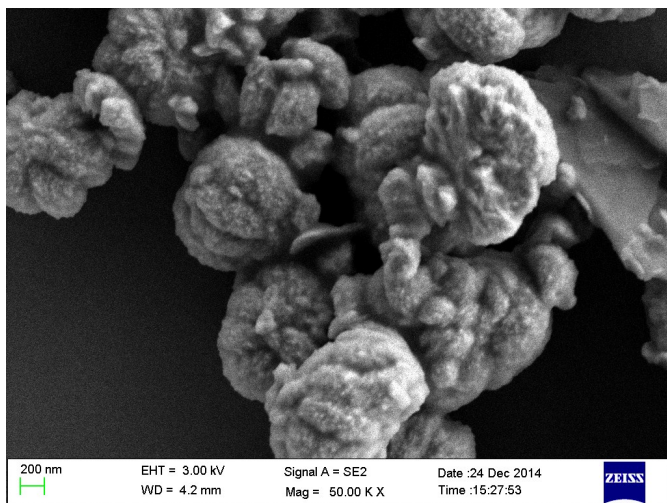


Figure 10. SEM image of CuO nanocatalyst showing microsphere morphology.

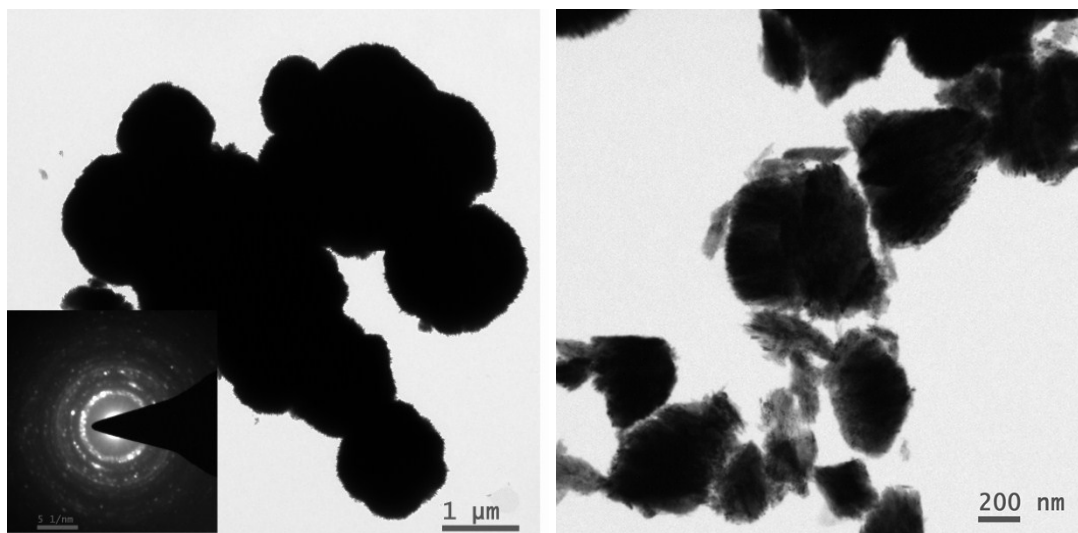


Figure 11. TEM image of CuO nano catalyst a) immediately after synthesis with electron diffraction pattern as inset b) after 1 hr sonication

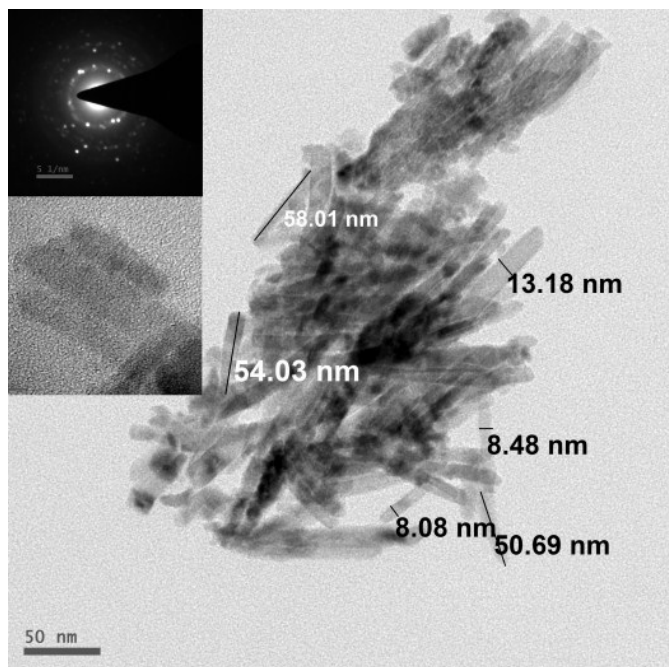


Figure 12. TEM image of CuO nanorods with electron diffraction pattern and HRTEM image as inset

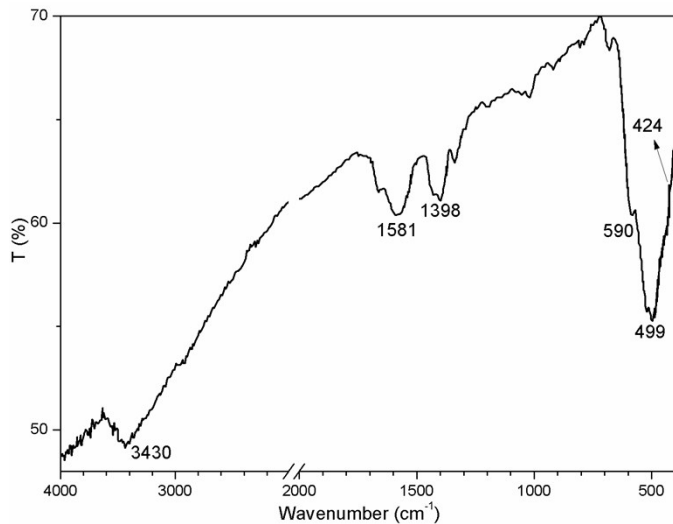


Figure 13: FTIR Spectrum of CuO nanorods

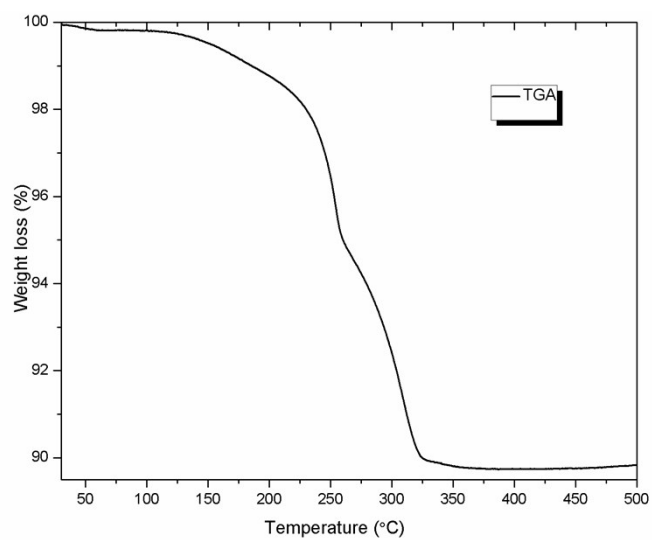


Figure 14: Thermogravimetric analysis of CuO